View metadata, citation and similar papers at core.ac.uk

brought to you by CORE

provided by DigitalCommons@University of Nebraska

University of Nebraska - Lincoln

DigitalCommons@University of Nebraska - Lincoln

Alexei Gruverman Publications

Research Papers in Physics and Astronomy

October 2003

Origin and implications of the observed rhombohedral phase in nominally tetragonal $Pb(Zr_{0.35}Ti_{0.65})O_3$ thin films

Paul C. McIntyre
Stanford University, pcm1@standford.edu

Alexei Gruverman
University of Nebraska-Lincoln, agruverman2@unl.edu

Bryan C. Hendrix
ATMI, Inc., Danbury, Connecticut

Steven M. Bilodeau
ATMI, Inc., Danbury, Connecticut

Jeffrey F. Roeder
ATMI, Inc., Danbury, Connecticut

Follow this and additional works at: https://digitalcommons.unl.edu/physicsgruverman

Part of the Physics Commons

McIntyre, Paul C.; Gruverman, Alexei; Hendrix, Bryan C.; Bilodeau, Steven M.; and Roeder, Jeffrey F., "Origin and implications of the observed rhombohedral phase in nominally tetragonal $Pb(Zr_{0.35}Ti_{0.65})O_3$ thin films" (2003). *Alexei Gruverman Publications*. 27.
https://digitalcommons.unl.edu/physicsgruverman/27

This Article is brought to you for free and open access by the Research Papers in Physics and Astronomy at DigitalCommons@University of Nebraska - Lincoln. It has been accepted for inclusion in Alexei Gruverman Publications by an authorized administrator of DigitalCommons@University of Nebraska - Lincoln.

JOURNAL OF APPLIED PHYSICS VOLUME 94, NUMBER 8 15 OCTOBER 2003

Origin and implications of the observed rhombohedral phase in nominally tetragonal $Pb(Zr_{0.35}Ti_{0.65})O_3$ thin films

Maxim B. Kelman[a] and Paul C. McIntyre[b]
Department of Materials Science and Engineering, Stanford University, Stanford, California 94305

Alexei Gruverman
Department of Materials Science and Engineering, North Carolina State University, Raleigh, North Carolina 27695

Bryan C. Hendrix, Steven M. Bilodeau, and Jeffrey F. Roeder
ATMI, Inc., 7 Commerce Drive, Danbury, Connecticut 06810

(Received 16 May 2003; accepted 28 July 2003)

The structural and electrical properties of $Pb(Zr_{0.35}Ti_{0.65})O_3$ (PZT) thin films ranging in thickness from 700 to 4000 Å have been investigated. These (001)/(100)-textured films were grown by metalorganic chemical vapor deposition on (111)-textured Ir bottom electrodes. It was observed that, in the as-deposited state, the thinnest PZT films are rhombohedral even though bulk PZT of this composition should be tetragonal. Thicker films have a layered structure with tetragonal PZT at the surface and rhombohedral PZT at the bottom electrode interface. In this article we investigate the origin of this structure and its effect of the ferroelectric and dielectric properties of PZT capacitors. It has been suggested that thin films stresses can affect the phase stability regions of single domain PZT. This possibility has been investigated by piezoresponse microscopy and thin film stress measurements. In the as-deposited state the majority of PZT grains contain a single ferroelastic domain, whereas after a high temperature anneal, a large fraction of the grains contain several ferroelastic domains. Wafer curvature measurements in combination with x-ray diffraction stress measurements in the Ir bottom electrode showed that the as-deposited PZT films are, within experimental error, stress free at room temperature. Landau–Ginbzurg–Devonshire formalism was used to explain the origin of the rhombohedral phase as a result of substrate constraint on single domain PZT grains. Annealing was found to affect the relative volume fractions of the rhombohedral and tetragonal phases and the electrical properties of PZT films. Intermediate temperature anneals increased the volume fraction of the rhombohedral phase and the coercive field extracted from the polarization-electric field hysteresis loops. After a high temperature anneal (650 °C) the majority of the grains transformed into a polydomain state, decreasing the volume fraction of the rhombohedral phase and the coercive field. If the high temperature anneal was performed after deposition of the top electrode, the coercive field became independent of the PZT thickness. © *2003 American Institute of Physics.* [DOI: 10.1063/1.1610773]

I. INTRODUCTION

Bulk ferroelectric $Pb(Zr_xTi_{1-x})O_3$ (PZT) ceramics have been investigated extensively in the past for their excellent piezoelectric properties.[1] More recently, thin films of PZT have been investigated for their applications in nonvolatile memories,[2] microelectromechanical system (MEMS) devices[3,4] and high frequency capacitors.[5] For nonvolatile memory applications, decreasing the thickness of the PZT should result, in principle, in a decrease in the operating voltage of the device while maintaining the same polarization characteristics. However, it has been observed in the past that decreasing the film thickness can, for example, change the domain structure and the lattice parameters[6] and increase the coercive field of the PZT. Several groups have reported that the coercive field of epitaxial and polycrystalline PZT films increases with a decrease in thickness,[6–8] while others have reported that it remains constant.[9] The increase in the coercive field of PZT with decreasing thickness has been attributed, for example, to a so-called ‘‘dead layer’’ or ‘‘blocking layer’’ at the ferroelectric/electrode interface that has a reduced dielectric constant.[7,10]

Our studies in the past have focused on the structural properties of PZT thin films with a Ti/Zr ratio of 65/35 and thicknesses of 700, 1000, 1500, 2500, and 4000 Å. While PZT of this composition should be tetragonal according to the bulk phase diagram,[1] it was observed that this is not the case for all PZT thin films in the thickness series. As-deposited PZT films 1000 Å and thinner were mostly rhombohedral,[11] whereas thicker PZT films had a layered structure with tetragonal PZT at the surface and rhombohedral PZT at the substrate interface.[12]

In this article we will attempt to explain the origin of the rhombohedral phase in nominally tetragonal PZT in terms of the different boundary conditions for PZT films compared to those for bulk ceramics, specifically stresses that might exist

[a]Electronic mail: maxkel@stanford.edu
[b]Electronic mail: pcm1@stanford.edu

 © 2003 American Institute of Physics

as a result of the deposition process and thermal cycling, and the constraints placed on PZT by constraint of the substrate. Implications of the observed structure on the ferroelectric and dielectric properties of these films will also be discussed.

II. EXPERIMENT

While details of sample characterization have been reported previously,[11,12] in the interest of completeness they will be summarized here. We have investigated the structural and electrical properties of polycrystalline PZT thin films deposited by metalorganic chemical vapor deposition (MOCVD) on Ir-electroded wafers.[13] Five different PZT film thicknesses were investigated ranging from 700 to 4000 Å. Cross-sectional scanning electron microscopy (SEM) showed that these films have a columnar microstructure with grains extending through the thickness of each film. Composition analysis by Rutherford backscattering spectrometry and x-ray fluorescence spectrometry showed that, within the resolution of each of these techniques (<1 at. %), the Ti to Zr ratio is approximately 65/35 and that $Pb/(Zr+Ti)=1$ for all PZT thicknesses and through the thickness of each film. Despite the compositional homogeneity of these films, high-resolution symmetric x-ray diffraction (XRD) showed that significant structural differences exist as the thickness of PZT changes. Electron backscatter diffraction, XRD, and electrical measurements showed that the thinnest as-deposited PZT films of 1000 Å and less are rhombohedral, while the thicker films are partially tetragonal and partially rhombohedral.[11] X-ray depth profiling using grazing incidence asymmetric Bragg geometry showed that the thicker as-deposited PZT films are tetragonal at the surface and rhombohedral at the substrate interface. For the 1500 Å thick PZT film, the thickness of the tetragonal layer at the surface was found to be approximately equal to the surface roughness of the film and thus corresponds to the topmost portion of the grains unconstrained by the surrounding film.[12] The layered structure of these PZT films can be used to explain the features observed in the symmetric x-ray diffraction pattern of the thicker PZT films, and it suggests that the layered structure we have observed for the PZT films of intermediate thickness exists in thicker films as well.

The structural properties of as-deposited and annealed PZT films reported in this study were investigated using symmetric x-ray diffraction measurements performed at Stanford Synchrotron Radiation Laboratory beamline 2-1. A monochromator was used to set the energy of the incident x rays to 7000 eV. An analyzer crystal between the sample and the detector limited divergence of the diffracted x rays and improved the signal to noise ratio of the measurements. Relative volume fractions of the rhombohedral and tetragonal phases were determined from the ratio of the integrated intensities of their peaks in symmetric XRD scans, which were analyzed by fitting all peaks with a Voigt function.

The stress in the as-deposited PZT films was determined using a combination of x-ray diffraction and wafer curvature techniques. The wafer curvature of Ir-electroded wafers was measured before and after PZT deposition using the Tencor Flexus FLX-2320. Asymmetric x-ray diffraction was used to measure stress in the (111)-textured Ir bottom electrode before and after PZT deposition. The change in spacing of the Ir (331)-type planes inclined with respect to the sample normal as a function of the their inclination angle Ψ can be related to the stress in the film using the $\sin^2\Psi$ method, as described in detail by a number of authors.[14–16]

Some of the samples were annealed for 30 min in flowing oxygen at temperatures ranging from 380 to 650 °C. In most cases, the PZT films were annealed prior to the deposition of top electrodes for electrical measurements. Capacitors were defined on blanket PZT films by e-beam evaporating Pt top electrodes through a shadow mask at room temperature. For most electrical measurements the capacitor areas ranged from 0.05 to 0.08 mm^2.

The dielectric properties of the PZT capacitors were measured either with a Hewlett-Packard 4284 meter (LCR) meter using a 100 mV AC ripple running at 10 kHz or using Evanescent Wave Microscopy operating at microwave frequencies (Ariel Technologies, Moraga, CA).[17–19] The ferroelectric properties of the capacitors were measured with a Sawyer–Tower circuit using a triangular wave form at 10 kHz with a maximum voltage of up to 10 V for the thickest PZT films.

Domain imaging of the films was performed by piezoresponse force microscopy (PFM). The PFM imaging method is based on the detection of local electromechanical displacement of a ferroelectric surface as a result of the converse piezoelectric effect. Typical experimental conditions used throughout the experiments can be summarized as follows. Standard Pt-coated Si cantilevers with spring constant of 2 N/m with a resonant frequency of about 38 kHz were used for domain imaging. During imaging, 10 kHz AC voltage was applied to the tip. The amplitude of the modulation voltage depended on the sample thickness and was in range of 0.5–1.0 V root mean square (rms).

III. RESULTS AND DISCUSSION

A. Origin of the rhombohedral phase

1. Piezoresponse imaging

A number of theories have been proposed to predict the effects of mechanical stress or substrate constraint on the phase stability regions of PZT thin films.[20–24] For example, the theoretical work of Pertsev *et al.*[21] on epitaxial single-domain $PbTiO_3$ thin films suggests that sufficiently high misfit tensile strain can transform tetragonal lead titanate into monoclinic phase. Similarly, Amin *et al.*[20] predicted that stress can shift the position of the morphotropic phase between tetragonal and rhombohedral phases in $Pb(Zr_{0.48}Ti_{0.52})O_3$. Since motion of 90° domain walls can accommodate the imposed, or misfit stress and strain[25,26] in order for these theories to be applicable to the polycrystalline PZT films investigated here, it is necessary for each grain of PZT to contain a single ferroelastic domain. We have previously proposed that this is the case for as-deposited films based on symmetric x-ray diffraction measurements of the PZT films of various thicknesses.[11,12]

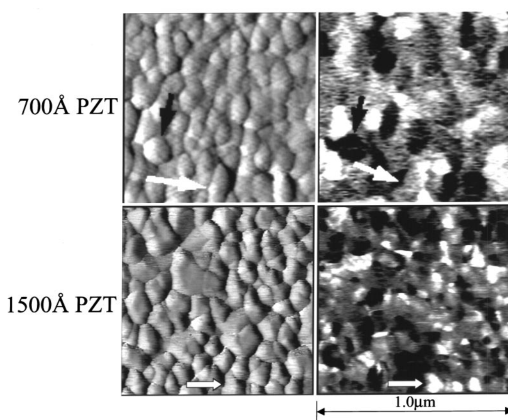

FIG. 1. Domain structure in 700 and 1500 Å as-deposited PZT. The image on the left shows the topography of the sample, while the image on the right side shows the piezoresponse signal. The arrows indicate single domain grains.

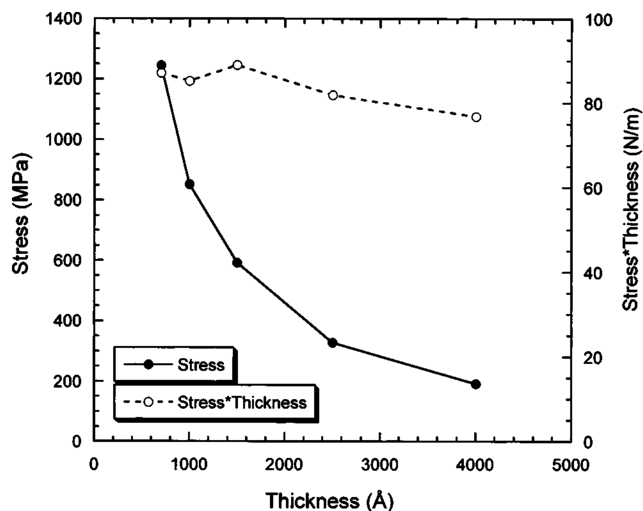

FIG. 2. Stress in PZT measured by wafer curvature before and after PZT deposition. The bending moment on the wafer is independent of the PZT thickness.

Piezoresponse microscopy[27–29] measurements were performed to confirm this experimentally for the 700 and 1500 Å films. For the thicker films, these measurements are complicated by the extreme roughness of the PZT surface. As shown in the cross-sectional SEM images we published previously,[11] PZT films thicker than 1500 Å are composed of columnar grains with sharp pyramidal tops. This affects the piezoresponse measurements because they require the contact between two very sharp tips: the atomic force microscope (AFM) tip and the tip of each grain.

Figure 1 shows the results of the piezoresponse measurements for 700 and 1500 Å as-deposited PZT films. The left side of the image shows the surface topography, whereas the right side of the image contains a combination of the phase and amplitude of the piezoresponse signal. The single contrast of the vast majority of grains suggests that, in the as-deposited state, each grain contains a single ferroelastic domain, that is, it does not contain any 90° domain walls. Since the lateral grain size of each grain does not change significantly with an increase in the thickness of PZT, it is reasonable to assume that the single domain nature of each grain is maintained for all PZT thicknesses in the as-deposited state.

2. Wafer curvature measurements

Since the as-deposited PZT films seem to be composed of single domain grains, the tetragonal to rhombohedral phase transformation observed may result from stress that appears in the film during PZT deposition or upon cooling from the deposition temperature. The stress in PZT can be calculated from the wafer curvature measurements performed before and after PZT deposition assuming the stress in the iridium bottom electrode does not change during deposition of the PZT. The validity of this assumption will be investigated in Sec. III A 3.

The results of the wafer curvature measurements are shown in Fig. 2. The apparent stress in PZT varies significantly as a function of the film thickness. It is very high for the thinnest PZT films and decreases as the PZT thickness increases. It is interesting to note that the stress in the PZT multiplied by the film thickness, or the bending moment and the resulting curvature of the substrate, are basically independent of the PZT film thickness. This observation can be accounted for by three different models: uniform stress in PZT that decreases from 1250 to 250 MPa as the PZT thickness increases from 700 to 4000 Å, a two layered model where the first PZT deposited is highly stressed and is rhombohedral and the remaining PZT is stress free and tetragonal, and a change in uniform biaxial stress in the iridium layer that is independent of the deposition time and PZT thickness. These possibilities were investigated by x-ray stress measurements of the Ir bottom electrode before and after PZT deposition.

3. Stress in the bottom electrode

As discussed in detail by Doerner and Nix[30] for thin films in general, significant growth and thermal stress can exist in the as-deposited iridium bottom electrode. Annealing the film can change the stress as a result of grain growth, dislocation motion, or film densification.[31,32] The stress in the bottom electrode can also change during the growth of PZT because it takes place at an elevated temperature of 570 °C in a highly oxidizing ambient.[11] While the stress evolution in an unpassivated as-deposited Ir film during a similar 570 °C anneal could in principle be measured using wafer curvature methods, that information would not be reliable for two reasons. As shown by Venkatraman *et al.* for aluminum films[33,34] or by Leung *et al.* for gold films,[35] the presence of a passivating layer, in this case PZT, on the surface of a metallic film can affect its stress evolution during annealing. The presence of PZT on the surface of the Ir bottom electrode might also affect its oxidation and the corresponding volume expansion. To avoid these effects, it is necessary to determine the stress in the Ir bottom electrode before and after high-temperature deposition of the PZT cap layer. This can be done using x-ray diffraction methods that allow for nondestructive investigation of stress in buried layers.

As discussed by Clemens and Bain,[14] a family of planes inclined with respect to the sample normal can be used to

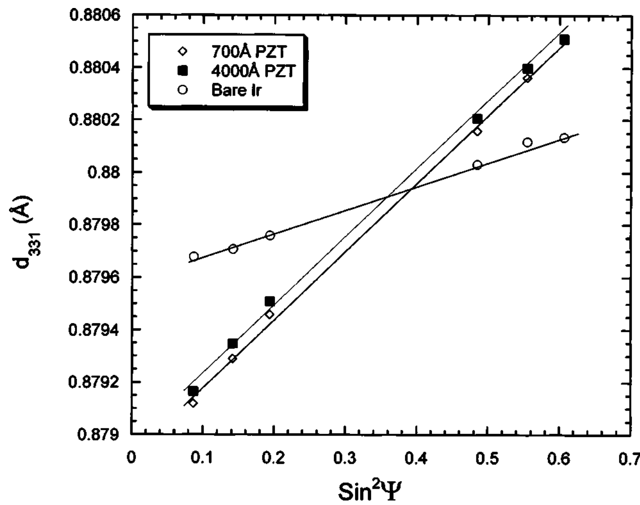

FIG. 3. Stress evolution in the Ir bottom electrode during PZT growth from x-ray diffraction $\sin^2\Psi$ measurements.

determine the biaxial strain in the film. In (111)-textured face-centered-cubic (fcc) films, the (331)-type planes that are inclined with respect to the sample normal by $\Psi=22°$ and $\Psi=48.5°$ (Ref. 14) satisfy this criterion. Because the iridium bottom electrodes used in this study are not perfectly (111) textured, inclination angles somewhat different from ideal values can also be used.

The results of the $\sin^2\Psi$ stress measurements[14,16] of the Ir bottom electrode before and after deposition of 700 and 4000 Å of PZT are shown in Fig. 3, which shows how the spacing of the Ir (331)-type planes changes as a function of their angle with respect to the sample normal. The slope of the line in Fig. 3 is proportional to the biaxial strain in the Ir film.[14] Clearly, the slope of this line increases during deposition of the first 700 Å of PZT. Since the slopes of the lines corresponding to Ir under 700 and 4000 Å PZT are equal, no additional strain evolution takes place in the bottom electrode during further growth of PZT.

To calculate the exact value of film stress that corresponds to the slope in the $\sin^2\Psi$ plot it is necessary to assume a specific texture for the Ir film. As we have discussed previously, the Ir bottom electrodes are mostly (111) oriented, with only those peaks present in the long-anguler range XRD scans. However, the bottom electrode is not very well textured, since the rocking curve of the symmetric peak is broad, with full width at half maximum intensity of approximately 15°.

For a fully (111)-textured film, the stress in Ir is equal to[14]

$$\sigma=\frac{2m}{d_0 S_{44}}, \tag{1}$$

where m is the slope of the line in Fig. 3, d_0 is the unstrained lattice spacing of the (331) planes and S_{44} (Ref. 36) is the anisotropic compliance constant. Following Eq. (1), the change in stress in Ir $(\Delta\sigma)$ can be related to the change in slope (Δm). Assuming the Ir bottom electrode is fully (111) textured, during deposition of the first 700 Å of PZT, the stress increases by 960 MPa.

For a randomly oriented film, the stress is equal to[16]

$$\sigma=\frac{mE}{(1+\nu)d_0}, \tag{2}$$

where E is the Young's modulus and ν is the Poisson ratio of the film.[37,38] Thus, for a fully random film the increase in the slope in Fig. 3 during PZT deposition corresponds to an increase in the tensile stress in the Ir bottom electrode by approximately 785 MPa.

As already mentioned, the degree of texture in the Ir bottom electrode is between fully (111) textured and randomly textured. Thus, the actual stress in the film that corresponds to the results shown in Fig. 3 is between 785 and 960 MPa, the calculated values for a fully (111)-textured and a randomly oriented film.

4. Stress in PZT

The increasing tensile stress in the Ir bottom electrode during deposition of the first 700 Å of PZT without further stress increases associated with increasing PZT thickness would result in a bending moment on the substrate that does not change for PZT thicker than 700 Å. This has been observed experimentally by wafer curvature measurements and shown in Fig. 2. The increase in stress in the 1000 Å thick Ir bottom electrode calculated from the wafer curvature measurements is equal to 851 MPa, which is between the value calculated for the fully (111)-textured and the fully random Ir film from XRD measurements. Thus, x-ray measurement of the change in stress in the Ir electrode can account for all of the changes in wafer curvature observed as a result of PZT deposition. Consequently, within the error of approximately ± 90 MPa associated with the imperfect texture of the Ir bottom electrode, the as-deposited PZT films are free of macroscopic stress, regardless of the PZT thickness.

5. Calculated stress in PZT grains

To understand the origin of the observed tetragonal to rhombohedral phase transformation consider a grain of 65/35 Ti/Zr PZT composed of a single ferroelastic domain. If the grain is not constrained by its surroundings it will spontaneously strain as it is cooled from the deposition temperature. For a (001)-oriented grain that was strain free at the deposition temperature, the in-plane strain will be equal to

$$\varepsilon^{c}_{\mathrm{PZT}}(T)=\frac{a_{\mathrm{PZT}}(T)-a_{\mathrm{PZT}}(T=T_{\mathrm{dep}})}{a_{\mathrm{PZT}}(T=T_{\mathrm{dep}})}+\sigma(S_{11}+S_{12}), \tag{3}$$

where a_{PZT} is the in-plane lattice parameter, T_{dep} is the deposition temperature, T is the temperature, σ is the biaxial stress, and S_{11} and S_{12} are the elastic compliance constants.

If this grain is attached to a thick Si substrate and surrounded by other PZT grains with random in-plane orientations, the position of the grain boundaries will be controlled by thermal expansion of the substrate. This situation is schematically depicted in Fig. 4. Since the thickness of the grain is significantly smaller than the thickness of the substrate, the in-plane strain in the grain will be equal to the strain in the substrate:

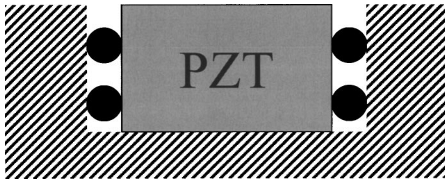

FIG. 4. Schematic of a single grain of PZT attached to a Si substrate.

$$\varepsilon_{\mathrm{Si}}(T)=\frac{a_{\mathrm{Si}}(T)-a_{\mathrm{Si}}(T=T_{\mathrm{dep}})}{a_{\mathrm{Si}}(T=T_{\mathrm{dep}})}. \tag{4}$$

If the film is constrained by the underlying substrate, the strain in the PZT ($\varepsilon^{c}_{\mathrm{PZT}}$) must equal the strain in the substrate ($\varepsilon_{\mathrm{Si}}$) at any temperature. Equations (3) and (4) can be solved simultaneously to determine the stress that arises in the PZT grain as it is cooled from the deposition temperature using thermal expansion data for Si,[39] lattice parameters for PZT with a very similar composition 68/32 Ti/Zr ratio,[40] and the elasticity constants of pure $PbTiO_3$.[41]

The same methodology can be applied to calculate the stress in the observed rhombohedral phase by assuming that its lattice parameter can be extrapolated from the lattice parameter of the cubic phase above the Curie temperature.

Unlike (001)-oriented grains, (100)-oriented tetragonal grains will possess two in-plane lattice parameters. Consequently, the grain will not be under equal biaxial stress. However, since the film is composed of a large number of randomly in-plane oriented (100)-type grains, we consider the effective in-plane lattice parameter of an *a*-type grain to be the average of the two in-plane lattice parameters.

The experimentally observed room temperature out-of plane lattice parameters of the rhombohedral and tetragonal phases of the 65/35 Ti/Zr PZT films can be extracted from symmetric x-ray diffraction scans of the 700 and 4000 Å thick PZT.[11] They can be compared to the lattice parameters of bulk polycrystalline PZT of very similar composition of 68/32 Ti/Zr, as investigated by Haun *et al.*[40] Figure 5 shows how the lattice parameters of the bulk and thin film PZT compare to each other. The measured lattice parameters of

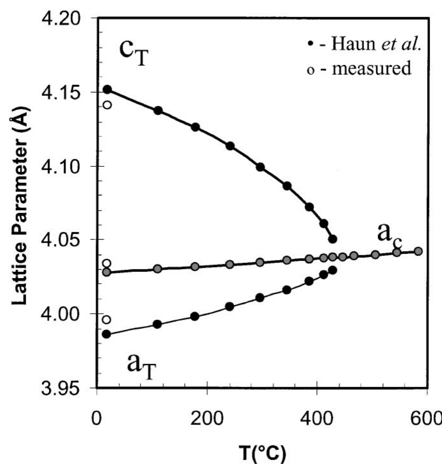

FIG. 5. Lattice parameters of bulk 68/32 PZT measured by Haun *et al.* (see Ref. 40) compared to the lattice parameters of the 65/35 PZT films measured in this study.

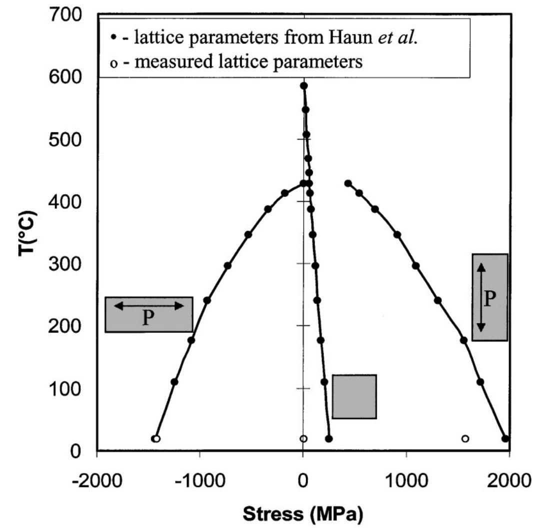

FIG. 6. Stress that would exist in a single ferroelastic domain grain of PZT calculated from its lattice parameter evolution with the temperature in comparison to thermal expansion of the silicon substrate.

tetragonal phase (c_T and a_T) are very close to the lattice parameters observed in bulk PZT. The slightly decreased tetragonality observed experimentally can be attributed to strain on the tetragonal phase that results from the layered structure of the thicker PZT films discussed in detail previously.[12] The observed room-temperature lattice parameter of the rhombohedral phase is also very close to the value of the lattice parameter of cubic phase extrapolated to room temperature.

As calculated from Eqs. (3) and (4), the stress that would exist in a PZT grain as it is cooled from the deposition temperature is shown in Fig. 6. If the transformation and thermal strain cannot be relieved by 90° domain wall motion as suggested by the piezoresponse measurements for the thinnest films, the *c*-type grains of tetragonal phase would be under very large biaxial tensile stress of up to 2 GPa. Similarly, the *a*-type grains of tetragonal phase would be under significant compression. The stress on a rhombohedral phase grain would be significantly smaller in comparison. If the lattice parameter extrapolated from the cubic phase is used, the predicted stress on a rhombohedral grain would be approximately 450 MPa. If the actually observed lattice parameter of the rhombohedral phase were used for the same calculations, the stress would be equal to approximately 18 MPa, which is consistent with the measured stress values as discussed in Sec. III A 4. As measured experimentally, the absence of macroscopic stress in the entire film is consistent with the predicted stress values for the thin PZT films composed entirely of rhombohedral phase. Thicker PZT grains with a layered structure containing tetragonal PZT at the surface should not contribute significantly to the macroscopic stress measured on the entire wafer for two reasons. First, if the film is composed of both variants of tetragonal phase, changing the relative volume fractions of the two phases can minimize stress in the entire film. Second, if tetragonal PZT exists only in parts of the grains unconstrained by their surroundings, the grains will be free to deform and accommodate the spontaneous strain resulting from the cubic to tetragonal phase transformation at the Curie temperature and

the subsequent cooldown. Thus the strain would not result in significant macroscopic stress in the film.

6. Landau–Ginzburg–Devonshire modeling

The effects of stress and strain on the phase stability regions in epitaxial single domain $PbTiO_3$ and PZT thin films have been modeled in the past using Landau–Ginzburg–Devonshire (LGD) theory by, for example, Pertsev *et al.*[21] and Oh and Jang.[23] They have shown that sufficiently high tensile stress can transform nominally tetragonal single domain $PbTiO_3$ into a monoclinic or a rhombohedral phase. We apply the theoretical framework developed by Haun *et al.*[42] for $PbTiO_3$ to investigate the effect of stress shown in Fig. 6 that would exist in single domain grains of tetragonal $Pb(Zr_{0.35}Ti_{0.65})O_3$ thin films on the stability of tetragonal PZT.

Following Haun *et al.*[42] the Gibbs free energy of PZT is expanded as a power series of the polarization.

$$\begin{aligned}\Delta G=&\alpha_1(P_1^2+P_2^2+P_3^2)+\alpha_{11}(P_1^4+P_2^4+P_3^4)\\&+\alpha_{12}(P_1^2P_2^2+P_2^2P_3^2+P_1^2P_3^2)+\alpha_{111}(P_1^6+P_2^6+P_3^6)\\&+\alpha_{112}[P_1^4(P_2^2+P_3^2)+P_2^4(P_1^2+P_3^2)+P_3^4(P_1^2+P_2^2)]\\&+\alpha_{113}P_1^2P_2^2P_3^2-\tfrac{1}{2}S_{11}(\sigma_1^2+\sigma_2^2+\sigma_3^2)-S_{12}(\sigma_1\sigma_2\\&+\sigma_2\sigma_3+\sigma_1\sigma_3)-\tfrac{1}{2}S_{44}(\sigma_4^2+\sigma_5^2+\sigma_6^2)\\&-Q_{11}(\sigma_1P_1^2+\sigma_2P_2^2+\sigma_3P_3^2)\\&-Q_{12}[\sigma_1(P_2^2+P_3^2)+\sigma_2(P_1^2+P_3^2)+\sigma_3(P_1^2+P_2^2)]\\&-Q_{44}(\sigma_4P_2P_3+\sigma_5P_1P_3+\sigma_6P_1P_2),\end{aligned}\tag{5}$$

where α_i, α_{ij}, and α_{ijk} are the dielectric stiffness constants, with α_i a function of the temperature, Q_{ij} and S_{ij} are the electrostriction and compliance constants, respectively, and P_i and σ_i are, respectively, the polarization and stress along the i direction. For the c-type tetragonal phase,

$$P_1=P_2=0,\quad P_3\neq 0,\tag{6}$$

whereas for the rhombohedral phase,

$$P_1^2=P_2^2=P_3^2\neq 0.\tag{7}$$

The Gibbs free energy of each phase is then obtained by substituting one of the two conditions of Eqs. (6) and (7) into the free energy expression in Eq. (5). The equilibrium polarization of the two phases can be calculated by minimizing the free energy in Eq. (5) with respect to the polarization,

$$\frac{\partial G}{\partial P_i}=0\Rightarrow P_i^0.\tag{8}$$

The equilibrium minimum free energy of each phase can then be found by substituting the P_i^0 values of each phase in the expression for free energy. These manipulations result in an expression for the Gibbs free energy of each phase as a function of the temperature and applied stresses σ_i. In thin films, the only nonzero components of the stress are σ_1, σ_2, and σ_6. For both the tetragonal and rhombohedral phases the two in-plane normal stress components will be equal to each other, i.e., $\sigma_1=\sigma_2=\sigma$. Since the tetragonal phase does not undergo in-plane shear distortion as it is cooled below the Curie temperature, the in-plane shear stress (σ_6) will be equal to zero as well. This is not necessarily the case for the rhombohedral phase. As discussed in detail by Corker *et al.*[43] and by Glazer *et al.*,[44,45] the rhombohedral phase of PZT has a very small spontaneous distortion along the (111) direction, resulting in spontaneous in-plane strain (ε_6). This distortion will be very small in magnitude, on the order of 0.2°–0.5°.[43] For these calculations, it is assumed that spontaneous in-plane distortion of the rhombohedral phase can be fully accommodated by grain-boundary motion during cooldown making the in-plane shear stress zero ($\sigma_6=0$).

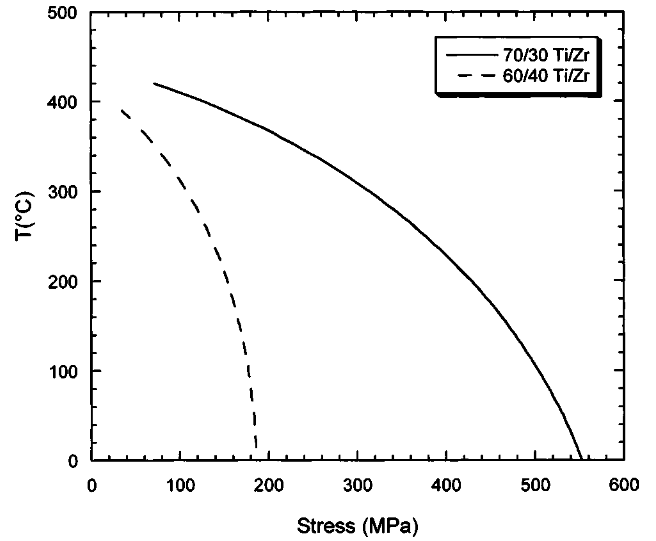

FIG. 7. Biaxial stress necessary for tetragonal to rhombohedral phase transformation calculated by the LGD model.

The manipulations described above result in an expression for the minimum free energies of tetragonal and rhombohedral phases as a function of several constants, the temperature and stress. Equating the two energies and solving for the stress gives the biaxial stress at which the two phases are energetically equally likely to exist. The rhombohedral phase is favorable for higher stress values, with the tetragonal phase stable at lower stresses. Since the electrostriction and dielectric stiffness constants are not available for the 65/35 Ti/Zr composition of the films we have investigated, the electrostriction and dielectric stiffness constant for PZT of very similar compositions of 70/30 and 60/40 Ti/Zr ratios from the work of Haun *et al.*[46] were used. The results of these calculations for temperatures below the Curie temperature are shown in Fig. 7.

As shown in Fig. 7, the biaxial stress necessary to transform grains containing a single ferroelastic domain from equilibrium tetragonal into the rhombohedral phase increases as the temperature is decreased below the Curie temperature. For c-type PZT grains with Ti/Zr ratios of 60/40 and 70/30, at room temperature the biaxial stresses reach approximately 200 and 550 MPa, respectively. This stress is significantly smaller than those that would exist in single domain c-type grains shown in Fig. 6. Relaxing the assumption that $\sigma_6=0$ increases the minimum biaxial stress necessary for tetragonal to rhombohedral phase transformation. However,

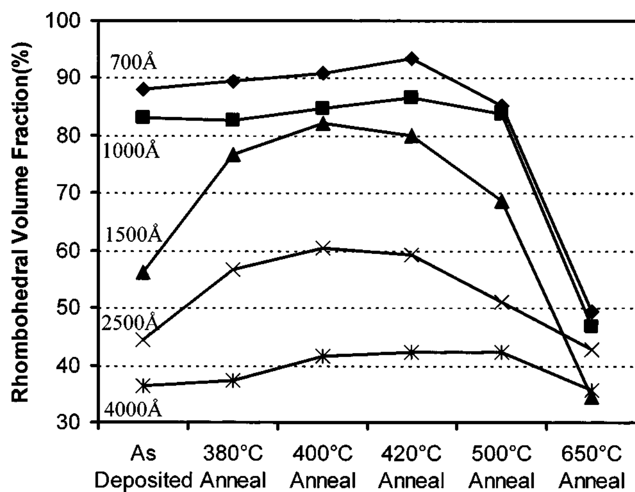

FIG. 8. Volume fraction of the rhombohedral phase as a function of the annealing treatment.

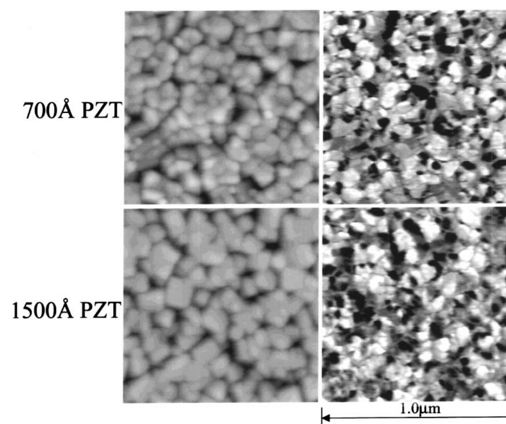

FIG. 9. Domain structure of 700 and 1500 Å PZT after the 650 °C anneal. The image on the left shows the topography of the sample, while the image on the right side shows the piezoresponse signal. A large fraction of grains appear to contain several ferroelastic domains.

that stress is still smaller than what would exist in single domain tetragonal PZT. Consequently, it is favorable for single domain PZT grains to transform into the rhombohedral phase instead of the tetragonal phase.

This analysis is consistent with the theoretical work recently published by Pertsev *et al.*[47] who investigated how the phase stability regions of PZT thin films of several compositions are affected by epitaxial misfit strain. They predicted that single domain PZT of 65/35 Ti/Zr ratio constrained by a substrate will not be tetragonal, but instead will be in monoclinic phase, with components of polarization both in the plane of the film and out of the plane of the film similar to what we have observed experimentally.

7. Annealing studies

The relative intensities of the tetragonal and rhombohedral peaks observed in symmetric XRD measurements change significantly with annealing treatment. The evolution of the volume fraction of rhombohedral phase as a function of the annealing temperature determined from symmetric x-ray diffraction measurements is shown in Fig. 8. At intermediate annealing temperatures, the relative volume fraction of the rhombohedral phase increases, as observed most clearly for intermediate thickness PZT films of 1500 and 2500 Å. As the annealing temperature increases further, the volume fraction of the rhombohedral phase decreases such that, after the 650 °C anneal, it becomes basically independent of the film thickness.

After the 650 °C anneal, the domain structure of PZT changes as evidenced by the piezoresponse microscopy images of annealed PZT films. As shown in Fig. 9, which contains topography and piezoresponse images of 700 and 1500 Å PZT films, a large number of grains contain regions of different piezoresponse contrast, suggesting that they have a polydomain structure.

The proposed origin of the tetragonal to rhombohedral phase transformation is consistent with the thickness-dependent phase transformation and the annealing experiments discussed. The pyramidal tops of the thicker grains are not constrained by the surrounding grains, allowing them to freely deform and accommodate the strain that develops upon cooling from the deposition temperature, including the transformation strain associated with the cubic to tetragonal phase transformation. This is consistent with the x-ray depth profiling measurements we have performed in the past, which showed that PZT has a layered structure with tetragonal phase at the surface and rhombohedral PZT is at the substrate interface.[12] As the films are annealed at intermediate temperatures, the film densifies by "zipping" the grain boundaries from the substrate interface. This increases the volume fraction of constrained PZT, which may then transform into the rhombohedral phase. The high-temperature anneals of 650 °C result in a large fraction of grains containing several ferroelastic domains. This is consistent with the work of Foster *et al.*[48] who showed that polydomain formation in epitaxial $PbTiO_3$ films can be affected by the annealing treatment. The formation of multiple ferroelastic domains within each grain allows them to maintain their overall shape during cooldown from the deposition temperature without the large deformations present in single domain grains. Consequently, after the high temperature anneal, films of all investigated thicknesses become mostly tetragonal. A stress-relieving transformation to the rhombohedral phase does not occur because another mechanism for stress accommodation is active.

B. Implications for electrical properties

1. Electrical properties of the as-deposited PZT films

The ferroelectric properties of the as-deposited PZT capacitors with unannealed Pt top electrodes were reported previously.[11] Similar to what has been observed by a number of other groups for epitaxial[6] and polycrystalline PZT,[7,8] the coercive field increases significantly with a decrease in thickness of PZT as shown in Fig. 10. It should be noted that some reports suggest the opposite. For example, Bilodeau *et al.*[9] showed that PZT films that were similarly deposited but annealed after top electrode deposition and patterning possess a coercive field that is independent of film thickness.

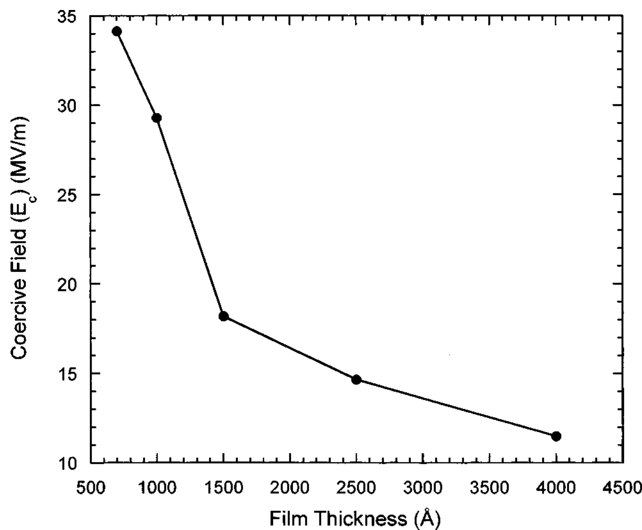

FIG. 10. Coercive field of as-deposited PZT thin films as a function of the film thickness.

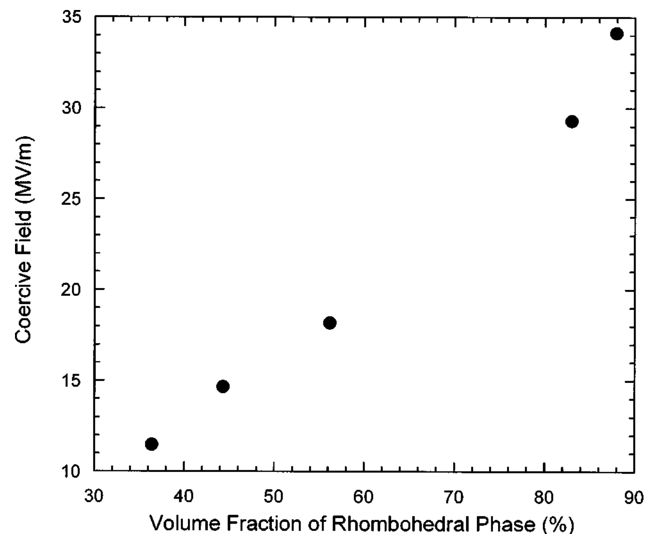

FIG. 12. Coercive field of as-deposited PZT films as a function of the volume fraction of the rhombohedral phase.

The increase in the coercive field of PZT with decreasing thickness has been attributed to, among others, a blocking or dead layer (mentioned earlier) at the ferroelectric/electrode interface that has a reduced dielectric constant.[7,10] The presence of an interfacial layer with a smaller dielectric constant would be manifested in a plot of the effective dielectric constant of PZT with increasing thickness. As discussed by Larsen *et al.*,[7] for nominally identical PZT films containing an interfacial layer the effective dielectric constant of the capacitor should asymptotically approach the bulk dielectric constant with an increase in thickness. As shown in Fig. 11 this is clearly not the case for the as-deposited PZT films as measured by the small signal capacitance at frequency of 10 kHz and by evanescent microwave probe at frequency of approximately 2 GHz. While the differences between the two sets of measured values can be attributed to the difficulty of extracting accurate values from the high-frequency measurements, the trend with thickness is very similar for both techniques. These results suggest that the structural evolution of PZT films with thickness affects their dielectric behavior. For example, the abrupt decrease in the dielectric constant for PZT 1500 Å thick coincides with transition of the film from mostly rhombohedral to a layered tetragonal/rhombohedral structure as we have discussed previously.[11,12] This observation is consistent with the theoretical prediction of Pertsev *et al.*[47] who showed that the dielectric constant of epitaxial PZT thin films changes abruptly as a result of the transformation from tetragonal into rhombohedral or monoclinic phase.

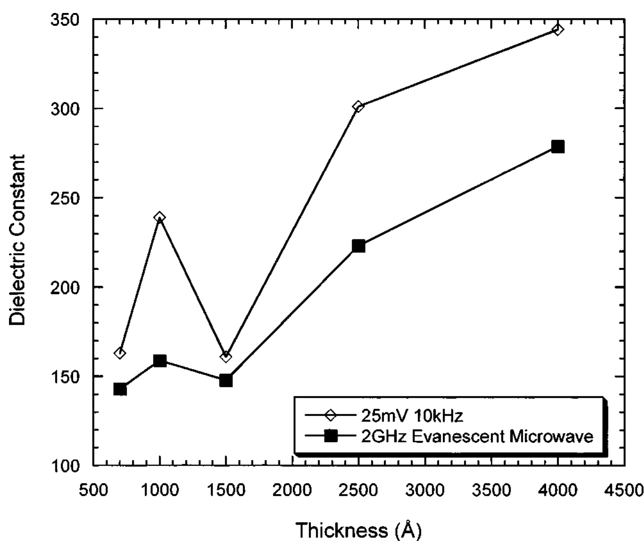

FIG. 11. Dielectric constant of as-deposited PZT films measured by small signal capacitance and evanescent microwave probe.

Since the increase in the coercive field of the as-deposited PZT films with decreasing thickness cannot be explained exclusively in terms of the dead layer at the electrode interfaces, it is reasonable to presume that the two-phase structure of PZT has an effect on its ferroelectric properties as well. Figure 12 shows how the coercive field of as-deposited PZT scales with the relative volume fraction of the rhombohedral phase determined by integrating the relative intensities of the peaks in symmetric XRD measurements. Clearly with increasing volume fraction of the rhombohedral phase the coercive field increases. This observation in itself is not sufficient to show that the increase in the coercive field with thickness is due exclusively to the increasing volume fraction of the rhombohedral phase, however, the annealing studies discussed in Sec. III B 2 of this article suggest that this is at least partially true.

The observation that the coercive field of PZT increases with an increase in volume fraction of the rhombohedral phase is contrary to what would be predicted based on experimental studies of PZT of several compositions. As shown by Foster *et al.* for epitaxial[49] and Hiboux *et al.* for polycrystalline PZT films,[50] the coercive field of rhombohedral PZT is lower than that of tetragonal PZT. However, those observations were made on PZT films that spanned the composition range from $PbTiO_3$ to $PbZrO_3$, whereas in this study we focus on PZT of a single composition that should be nominally tetragonal. One possible reason why the coercive field

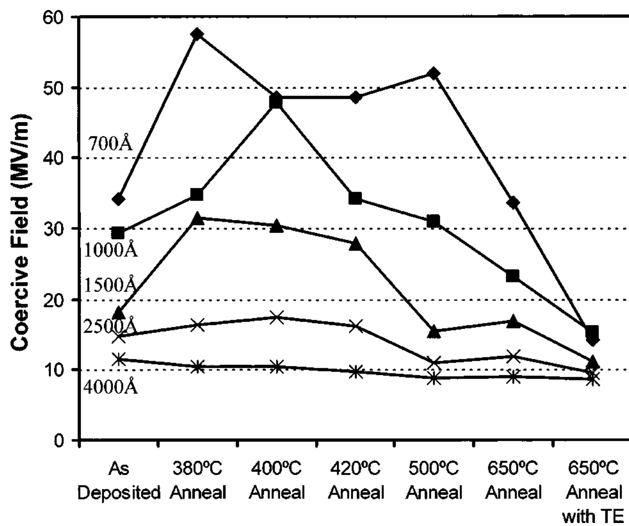

FIG. 13. Coercive field of PZT as a function of the annealing treatment.

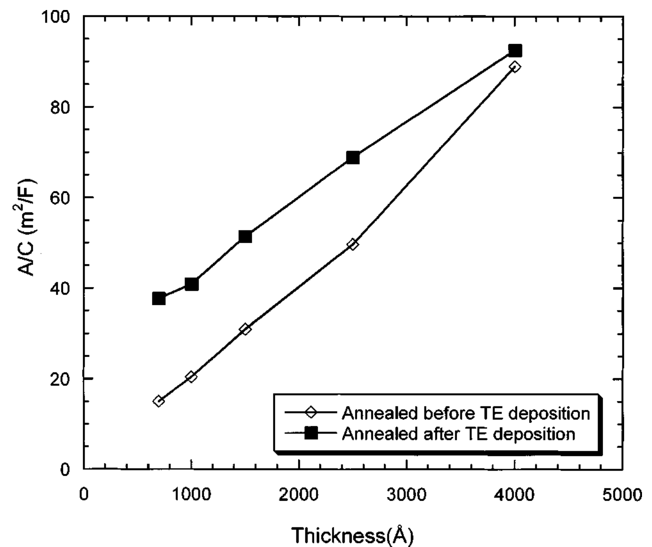

FIG. 14. Inverse capacitance of PZT films annealed at 650 °C for 30 min before and after deposition of the top electrode.

of the rhombohedral phase is higher than that of tetragonal PZT is that in the rhombohedral phase the polarization vector is parallel to the (111) direction, whereas the electric field is applied along the (001) direction.

2. Annealing studies

The ferroelectric properties of annealed PZT capacitors were measured to investigate whether the changes in relative volume fraction of the tetragonal and rhombohedral phases shown in Fig. 8 affect the coercive field of the films as suggested by the plot in Fig. 12. To eliminate the effects of electrode annealing on the electrical properties of PZT, most of the films were annealed prior to room temperature deposition of the Pt top electrode. Only one set of samples was annealed at 650 °C after deposition of the top electrode. As shown in Fig. 13, intermediate temperature anneals ($\sim$400 °C) increase the coercive field of all PZT films, correlating to the increase in the volume fraction of the rhombohedral phase for the same anneals. Higher temperature anneals ($T>500\,^{\circ}$C) decrease the volume fraction of the rhombohedral phase while also decreasing the coercive field. If a high temperature anneal of 650 °C is performed after deposition of the top electrode, the coercive field becomes independent of the PZT film thickness. This is not the case for films that were annealed prior to deposition of the top electrode. The differences in coercive field of the two sets of samples are a result of interfacial capacitance.

Figure 14 shows the dielectric properties of PZT capacitors 650 °C annealed before and after deposition of the Pt top electrode. The slope of the inverse capacitance versus thickness plot is proportional to the inverse of the dielectric constant of the bulk of the film,[7] whereas the intercept corresponds to the interfacial capacitance. Annealing the sample before or after deposition of the top electrode does not significantly alter the apparent bulk dielectric constant of PZT film but does remove the interfacial capacitance, making the coercive field thickness independent. These results further confirm that the changes in dielectric constant of as-deposited PZT films with the thickness shown in Fig. 11 are a result of structural differences present in the thickness series of the PZT films we have investigated.

IV. CONCLUSIONS

We have investigated the origin and implications of the tetragonal to rhombohedral phase transformation observed in nominally tetragonal $Pb(Zr_{0.35}Ti_{0.65})O_3$ thin films of varying thickness, where PZT films thinner than 1500 Å have a rhombohedral crystal structure and thicker films have a layered structure, with the tetragonal phase present in a layer near the film surface and the rhombohedral phase at the bottom electrode interface.

It has been suggested in the past that macroscopic stress on single domain PZT films can result in the presence of phases that are not expected in unstrained samples, such as the observed rhombohedral phase. Piezoresponse microscopy measurements suggest that in the as-deposited state the majority of PZT grains contain a single ferroelastic domain. Wafer curvature and x-ray stress measurements showed that, in the as-deposited state, there is no significant macroscopic stress in these films. The origin of the rhombohedral phase can be explained by considering the effect of substrate constraint on PZT grains. If the cubic to tetragonal transformation strain cannot be relieved by ferroelastic domain formation within each grain, the PZT grain would be under significant mechanical stress. This stress is more than sufficient to transform the equilibrium tetragonal phase into the rhombohedral phase as calculated by LGD theory.

It was observed that the structural properties of these PZT films affect their dielectric and ferroelectric properties. The coercive field in the as-deposited films scales with the volume fraction of rhombohedral PZT calculated from symmetric x-ray diffraction measurements. Similar trends were observed during postdeposition annealing experiments. Intermediate temperature anneals increased the volume fraction of the rhombohedral phase, while higher temperature anneals

(>500 °C) decreased both the volume fraction of the rhombohedral phase and the coercive field. After a 650 °C anneal, a large fraction of the grains are in a polydomain state, allowing them to relax to tetragonal phase and resulting in a coercive field that is thickness independent for films that are annealed after deposition of the top electrode. The high temperature anneal also removes certain anomalies in the thickness dependence of the dielectric behavior of as-deposited PZT films, which may be attributed to the tetragonal to rhombohedral phase transformation. If the high temperature anneal is performed after deposition of a Pt top electrode, it also removes interfacial capacitance, resulting in a coercive field that is thickness independent.

ACKNOWLEDGMENTS

This research was funded in part by the Fannie and John Hertz Foundation and the National Science Foundation Grant Nos. DMR9974341, DMR0205949, and DMR0235632. Portions of this research were carried out at the Stanford Synchrotron Radiation Laboratory, a national user facility operated by Stanford University on behalf of the U.S. Department of Energy, Office of Basic Energy Sciences.

[1] B. Jaffe, W. R. Cook, Jr., and H. Jaffe, *Piezoelectric Ceramics* (Academic, London, 1971).
[2] S. R. Summerfelt *et al.*, Appl. Phys. Lett. **79**, 4004 (2001).
[3] L. P. Wang, K. Deng, L. Zou, R. Wolf, R. J. Davis, and S. Trolier-McKinstry, IEEE Electron Device Lett. **23**, 182 (2002).
[4] P. Muralt, Integr. Ferroelectr. **17**, 297 (1997).
[5] D. Dimos and C. H. Mueller, Annu. Rev. Mater. Sci. **28**, 397 (1998).
[6] V. Nagarajan, I. G. Jenkins, S. P. Alpay, H. Li, S. Aggarwal, L. Salamanca-Riba, A. L. Roytburd, and R. Ramesh, J. Appl. Phys. **86**, 595 (1999).
[7] P. K. Larsen, G. J. M. Dormans, D. J. Taylor, and P. J. Van Veldhoven, J. Appl. Phys. **76**, 2405 (1994).
[8] J. F. M. Cillessen, M. W. J. Prins, and R. M. Wolf, J. Appl. Phys. **86**, 2777 (1997).
[9] S. M. Bilodeau, S. T. Johnston, M. W. Russell, D. J. Vestyck, and P. C. van Buskirk, Integr. Ferroelectr. **26**, 119 (1999).
[10] C. Zhou and D. M. Newns, J. Appl. Phys. **82**, 3081 (1997).
[11] M. B. Kelman, L. F. Schloss, P. C. McIntyre, B. C. Hendrix, S. M. Bilodeau, and J. F. Roeder, Appl. Phys. Lett. **80**, 1258 (2002).
[12] M. B. Kelman, P. C. McIntyre, B. C. Hendrix, S. M. Bilodeau, J. F. Roeder, and S. Brennan, J. Mater. Res. **18**, 173 (2003).
[13] J. F. Roeder, T. H. Baum, S. M. Bilodeau, G. T. Stauf, C. Ragaglia, M. W. Russell, and P. C. V. Buskirk, Adv. Mater. Opt. Electron. **10**, 145 (2000).
[14] B. M. Clemens and J. A. Bain, MRS Bull. **17**, 46 (1992).
[15] B. D. Cullity, *Elements of X-ray Diffraction*, 2nd ed. (Addison–Wesley, Reading, MA, 1978).
[16] I. C. Noyan and J. B. Cohen, *Residual Stress: Measurement by Diffraction and Interpretation* (Springer, New York, 1987).
[17] C. Gao, T. Wei, F. Duewer, Y. L. Lu, and X. D. Xiang, Appl. Phys. Lett. **71**, 1872 (1997).
[18] Y. L. Lu, T. Wei, F. Duewer, Y. Q. Lu, N. B. Ming, P. G. Schultz, and X. D. Xiang, Science **276**, 2004 (1997).
[19] C. Gao and X. D. Xiang, Rev. Sci. Instrum. **69**, 3846 (1998).
[20] A. Amin, R. E. Newnham, and L. E. Cross, Phys. Rev. B **34**, 1595 (1986).
[21] N. A. Pertsev, A. G. Zembiglotov, and A. K. Tagantsev, Phys. Rev. Lett. **80**, 1988 (1998).
[22] S. B. Desu, Z. J. Chen, V. P. Dudkevich, P. V. Dudkevich, I. N. Zakharchenko, and G. L. Kushlyan, in *Ferroelectric Thin Films V*, edited by S. B. Desu, R. Ramesh, B. A. Tuttle, R. E. Jones, and I. K. Yoo (Materials Research Society, Pittsburgh, PA, 1996), Vol. 433, p. 345.
[23] S. H. Oh and H. M. Jang, Appl. Phys. Lett. **72**, 1457 (1998).
[24] N. J. Ramer, S. P. Lewis, E. J. Mele, and A. M. Rappe, AIP Conf. Proc. **436**, 156 (1998).
[25] M. B. Kelman, P. C. McIntyre, B. C. Hendrix, S. M. Bilodeau, and J. F. Roeder, J. Appl. Phys. **93**, 9231 (2003).
[26] S. B. Ren, C. J. Lu, H. M. Shen, and Y. N. Wang, Phys. Rev. B **55**, 3485 (1997).
[27] A. Gruverman, O. Auciello, and H. Tokumoto, Annu. Rev. Mater. Sci. **28**, 101 (1998).
[28] A. Gruverman, A. Kholkin, A. Kingon, and H. Tokumoto, Appl. Phys. Lett. **78**, 2751 (2001).
[29] C. S. Ganpule *et al.*, J. Appl. Phys. **91**, 1477 (2002).
[30] M. F. Doerner and W. D. Nix, CRC Crit. Rev. Solid State Mater. Sci. **14**, 225 (1988).
[31] W. D. Nix, Metall. Trans. A **20A**, 2217 (1989).
[32] C. V. Thompson, Annu. Rev. Mater. Sci. **30**, 159 (2000).
[33] R. Venkatraman, J. C. Bravman, W. D. Nix, P. W. Davies, P. A. Flinn, and D. B. Fraser, J. Electron. Mater. **19**, 1231 (1990).
[34] R. Venkatraman and J. C. Bravman, J. Mater. Res. **7**, 2040 (1992).
[35] O. S. Leung, A. Munkholm, S. Brennan, and W. D. Nix, J. Appl. Phys. **88**, 1389 (2000).
[36] D. R. Lide, *CRC Handbook of Chemistry and Physics*, 75th ed. (Chemical Rubber, Boca Raton, FL, 1994).
[37] C. R. Barrett, W. D. Nix, and A. S. Tetelman, *The Principles of Engineering Materials* (Prentice–Hall, Englewood Cliffs, NJ, 1973).
[38] T. H. Courtney, *Mechanical Behavior of Materials* (McGraw–Hill, New York, 1990).
[39] Y. S. Touloukian, R. K. Kirby, R. E. Taylor, and T. Y. R. Lee, *Thermal Expansion-Nonmetallic Solids* (IFI/Plenum, New York, 1977).
[40] M. J. Haun, E. Furman, H. A. McKinstry, and L. E. Cross, Ferroelectrics **99**, 27 (1989).
[41] I. Ueda, S. Kobayashi, and S. Ikegami, National Technical Report **18**, 413 (1972).
[42] M. J. Haun, E. Furman, S. J. Jang, H. A. McKinstry, and L. E. Cross, J. Appl. Phys. **62**, 3331 (1987).
[43] D. L. Corker, A. M. Glazer, R. W. Whatmore, A. Stallard, and F. Fauth, J. Phys.: Condens. Matter **10**, 6251 (1998).
[44] A. M. Glazer, Acta Crystallogr., Sect. B: Struct. Crystallogr. Cryst. Chem. **B28**, 3384 (1972).
[45] A. M. Glazer, S. A. Mabud, and R. Clarke, Acta Crystallogr., Sect. B: Struct. Crystallogr. Cryst. Chem. **B34**, 1060 (1978).
[46] M. J. Haun, Z. Q. Zhuang, E. Furman, S. J. Jang, and L. E. Cross, Ferroelectrics **99**, 45 (1989).
[47] N. A. Pertsev, V. G. Kukhar, H. Kohlstedt, and R. Waser, Phys. Rev. B **67**, 054107 (2003).
[48] C. M. Foster, W. Pompe, A. C. Daykin, and J. S. Speck, J. Appl. Phys. **79**, 1405 (1996).
[49] C. M. Foster, G. R. Bai, R. Csencsits, J. Vetrone, R. Jammy, L. A. Wills, E. Carr, and J. Amano, J. Appl. Phys. **81**, 2349 (1997).
[50] S. Hiboux, P. Muralt, and T. Maeder, J. Mater. Res. **14**, 4307 (1999).